

Atomic and electronic structure of polymer organic semiconductors: P3HT, PQT, and PBTTT

John E. Northrup

Palo Alto Research Center, 3333 Coyote Hill Road, Palo Alto, California 94304, USA

(Received 30 April 2007; revised manuscript received 4 September 2007; published 13 December 2007)

First-principles pseudopotential density functional calculations were employed to investigate the atomic structure of three organic semiconductors: poly[5,5'-bis(3-alkyl-2-thienyl)-2,2'-bithiophene] (PQT), poly[2,5-bis(3-alkylthiophen-2-yl)thieno(3,2-b)thiophene] (PBTTT), and poly(3-hexylthiophene) (P3HT). The calculations show that a substantial rotation of the conjugated planes around the polymer axis is energetically favorable for all three crystals. This rotation reduces the overlap of molecular orbitals, and therefore increases the effective mass in the π - π stacking direction. This impacts the mobility, which is estimated within an acoustic deformation potential model. Similar values for the effective mass and mobility were obtained for P3HT and PBTTT. Therefore, the higher mobility observed experimentally for PBTTT in comparison to P3HT could be a result of improved structural ordering rather than being an intrinsic property of crystalline regions of the polymer. Calculations indicate that substantial interdigitation of the alkyl side chains is energetically favorable for PBTTT.

DOI: 10.1103/PhysRevB.76.245202

PACS number(s): 61.66.Hq, 72.80.Le

I. INTRODUCTION

Insight into the electronic and structural properties of two-dimensional sheets of conjugated polymers such as poly(3-hexylthiophene) (P3HT), poly[5,5'-bis(3-alkyl-2-thienyl)-2,2'-bithiophene] (PQT), and poly[2,5-bis(3-alkylthiophen-2-yl)thieno(3,2-b)thiophene] (PBTTT) has been the target of many recent investigations.¹⁻¹⁴ These semiconducting polythiophene materials are interesting because of their relatively high mobility coupled with solution processibility, allowing large area electronics and optoelectronics on mechanically flexible substrates at low cost.²⁻⁵ A greater degree of structural ordering is expected to increase the carrier delocalization, and result in an increase in the mobility.^{2,3} Consequently, a proper understanding of the factors which govern the atomic and electronic structure will be valuable in guiding the synthesis of new polymers.^{4,5} Enhanced mesoscopic ordering increases the mobility by reducing the fraction of disordered material between crystalline grains.⁹ In addition, improvement in the design of the material on the atomic scale can lead to higher mobility within a crystalline region.

The polymer crystals studied here exhibit a layered structure in which the polymer chains run in the [001] direction and are separated in the [010] direction from neighboring chains by a distance b , which is equal to about 3.8 Å.^{2,4,5} The polymers order into two-dimensional sheets, or lamellas. These lamellas are separated in the [100] direction from their neighbors by a distance (d) that is governed by the length of alkyl side chains (C_nH_{2n+1}). The number of C atoms in the alkyl side chain is chosen such that the polymer is soluble, and can be solution processed onto a substrate. Typical values of the chain length (n) employed in solution-processed material range between 6 and 16. The atomic structure viewed along the [010] direction is illustrated schematically for P3HT and PQT-C6 in Fig. 1.

As shown in Fig. 1, the difference between P3HT and PQT-C6 is defined by the density and arrangement of the side chains. In PQT-C6 the side chain density is lower by a factor of 2 in comparison to P3HT, and the length of the c

axis is twice as long in PQT. The alkyl side chains are attached in a head-to-tail arrangement in P3HT and in a head-to-head fashion in PQT.

The structure of PBTTT is illustrated in Fig. 2. Each monomer comprises two thiophene rings and one fused ring.⁵ There are two alkyl side chains (C_n) attached in a head-to-head arrangement on neighboring thiophene rings. By comparing the structures shown in Figs. 1 and 2, one sees that PBTTT can be obtained from PQT by removing two C atoms per monomer and fusing the thiophene rings. The structure shown in Fig. 2 has side chains with six carbon atoms. We therefore refer to this as PBTTT-C6.

In recent work the polymer series PBTTT-C $_n$ was reported to exhibit field-effect mobility in the range of 0.2–0.6 cm²/(Vs).⁵ This result has given rise to considerable interest in PBTTT-C $_n$ because these mobilities are greater than those seen in P3HT (Refs. 2 and 3) and PQT-C12.^{4,8} The mobility in those materials is typically measured to be less than or equal to 0.1 cm²/(Vs). Our objective in investigating the atomic and electronic structure of the materials is to gain

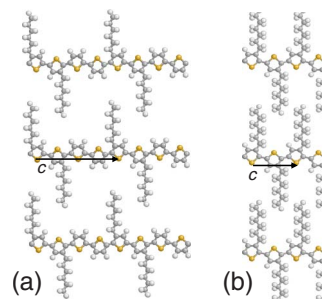


FIG. 1. (Color online) (a) Atomic structure of regioregular PQT-C6. (b) Atomic structure of regioregular P3HT. The all-trans side chains are attached in a head-to-head pattern in PQT and in a head-to-tail pattern in P3HT. The sulfur atoms (twofold coordinated) are yellow. The c axis is twice as long for PQT, and the density of alkyl chains is one-half that of P3HT. The degree of side-chain interdigitation depicted in these two structures has not been calculated, and is not necessarily optimal.

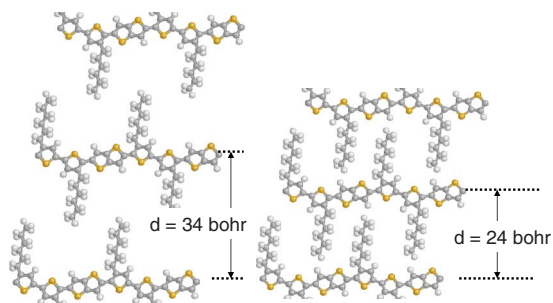


FIG. 2. (Color online) Atomic structure for PBTTT-C6 for two different d spacings. The energy vs d spacing is shown in Fig. 6. The fully interdigitated structure, with d spacing=24 bohr, has a lower energy.

insight into the reasons for the difference in mobilities of these materials.

In recent calculations for two-dimensional polythiophene sheets a significant rotation of the polymer backbone was predicted to be energetically favorable.^{7,9} This rotation, or tilt, is defined in Fig. 3. This tilt is important because it governs the interaction between neighboring chains, and therefore has a significant effect on the band structure and optical properties of the material. The initial calculations were carried out for a generic polythiophene model, in which the alkyl side chains were replaced by H atoms.⁹ Subsequent calculations of the rotation angle for PBTTT employed CH₃ groups to represent the side chains.⁷ A substantial rotation ($\sim 27^\circ$) was predicted in that case also. Experiments employing near-edge x-ray-absorption fine-structure (NEXAFS) spectroscopy have confirmed the tilt; the measured value is $\sim 21^\circ$ for PBTTT-C14.⁷

In the present paper we report calculations for polythiophene sheets with alkyl side chains containing six C atoms. The rotation of the backbone is energetically favorable in this case also. Substantial backbone rotation appears to be a general feature of this type of crystalline polymer. We also report the results of calculations of the electronic structure for PBTTT and P3HT, and employ these results to provide estimates of the hole mobility based on the acoustic deformation model of scattering. The estimates suggest that the superior effective mobility measured in devices employing

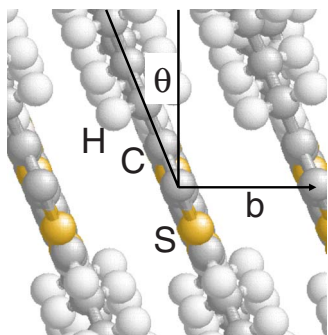


FIG. 3. (Color online) View of PBTTT along the c axis, showing the definition of the tilt angle θ . The lattice vector \mathbf{b} points in the π - π stacking direction.

PBTTT is not a consequence of an intrinsically higher mobility within crystalline regions. Finally, we investigate the energy of interdigitation of the side chains in PBTTT. The results show that interdigitation is energetically favorable, in agreement with recent experiments.⁷

II. METHOD

The total energy calculations employed pseudopotential density functional theory with a plane wave basis having a cutoff energy of 40 Ry. Troullier-Martins pseudopotentials are adopted for the S and C atoms, while the exact $1/r$ potential is employed for the H atoms. Forces are calculated and employed to determine the atomic positions corresponding to local minima in the total energy. The local density approximation corresponding to the Ceperley-Alder correlation functional was used.¹⁵⁻¹⁸ This approach has been employed previously in investigations of pentacene to calculate surface energies and defect energies.^{19,20} The calculations,¹⁹ which employed experimentally determined lattice constants, predicted an equilibrium crystal shape of pentacene that is very close to crystal shapes seen in experiment.²¹

Except where noted below, the calculations employ orthorhombic unit cells with lattice vectors $\mathbf{a}=(d,0,0)$, $\mathbf{b}=(0,b,0)$, and $\mathbf{c}=(0,0,c)$. The distance between neighboring sheets (d) is taken to be sufficiently large to reduce interaction between interdigitated alkyl chains of the neighboring sheets. The lengths of the in-plane lattice vectors \mathbf{b} and \mathbf{c} are determined by energy minimization. For PBTTT-C6 we find $b=7.1$ bohr (3.8 Å) and $c=25.5$ bohr (13.5 Å). For P3HT we find $b=7.1$ bohr (3.8 Å) and $c=14.4$ bohr (7.6 Å). X-ray-diffraction experiments for PBTTT-C14 indicate a π -stacking distance $b=3.72$ Å, equal to 7.03 bohr.⁵ The excellent agreement between theory and experiment provides support for the use of the local density approximation to describe the interaction between neighboring polythiophene chains.

To obtain an estimate of the accuracy of the LDA for describing the weak interaction between π -stacked molecules we performed test calculations on the benzene dimer in the parallel-displaced geometry. This structure consists of two benzene rings (C_6H_6) that are displaced relative to each other by R_1 in the direction orthogonal to the rings, and R_2 along a line in the plane of the rings that passes through the center of a ring and the midpoint of one of the C-C bonds. Our LDA energy minimization calculations give $R_1=3.28$ Å and $R_2=1.65$ Å. This corresponds to a distance of 3.67 Å between the centers of mass of the two rings, and a tilt angle $\varphi=\tan^{-1}(R_2/R_1)$ of 26.7° . For comparison, a recent quantum chemistry calculation, expected to provide a very accurate treatment of electron correlation, gives $R_1=3.4$ Å and $R_2=1.6$ Å.²² The corresponding distance and angle are 3.76 Å and 25.2° . The comparison suggests that the expected accuracy for our lattice constant (b) is about 0.1 Å, and the accuracy of the tilt angle of the planes containing the rings is $\sim 2^\circ$.

In a recent study of bulk anthracene ($C_{14}H_{10}$), the local density approximation was employed to determine the orientation of the molecules as a function of pressure.²³ An excel-

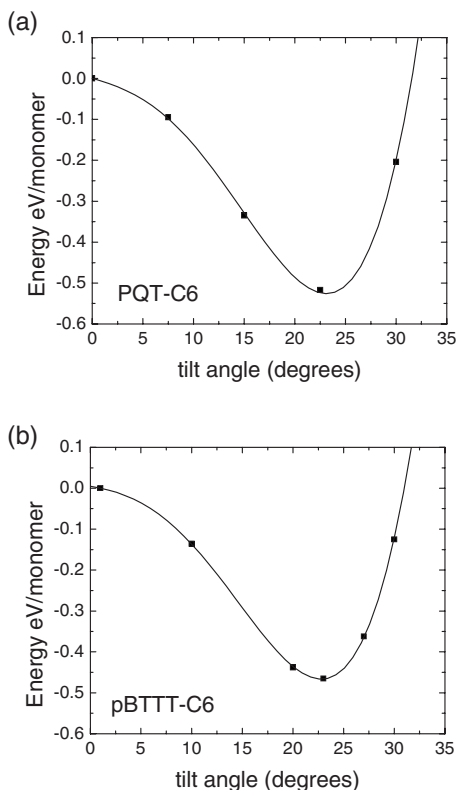


FIG. 4. The energy vs tilt angle is shown for PQT-C6 and PBTTT-C6. The crystalline material exhibits a local maximum in energy (an instability) for $\theta=0$. The minimum energy occurs for $\theta=23^\circ$. The energy reduction arising from the rotation is on the order of 0.1 eV per sulfur atom.

lent agreement between theoretical and experimental values of the orientation angles was obtained. Anthracene is a prototypical π -stacked molecular crystal in which there is hybridization of the molecular orbitals on neighboring molecules. In this respect it is similar to the polythiophene crystals studied here, where there exists a significant electron density in the interstitial regions, arising from interaction between C and S orbitals on neighboring polymer chains. One may expect therefore that tilt angles of the polymer chains can be given accurately by local density calculations.

III. RESULTS

A. Tilt of the backbone

The total energy was calculated for PBTTT-C6 and PQT-C6 as a function of the tilt angle of the conjugated backbone and the results are shown in Fig. 4. It is seen immediately that tilting is energetically favorable; the structure with no tilt, $\theta=0$, is a *local maximum* in the energy. The minimum in energy occurs for an angle of about 23° in both cases. The energy reduction arising from the rotation is substantial; it is 0.46 eV/monomer for PBTTT-C6, and 0.52 eV/monomer for PQT-C6. This result for PBTTT-C6 confirms prior investigations for PBTTT-C1, where we considered a model in which the side chains are replaced by methyl groups, and found an equilibrium rotation angle of

27° and an energy reduction of 0.35 eV/monomer.⁷ It is clear that there is a substantial driving force for the tilting of the conjugated chains.

B. Electronic structure

Interaction between polymer chains, and the possibility of hole delocalization, is widely recognized to play an important role in the charge transport properties of thin films of conjugated polymers.²⁻¹⁴ It is therefore important to investigate and compare the band structure of these two-dimensional materials. Effective masses extracted from the calculations can be employed to estimate the mobility.

In these types of conjugated π systems the position in \mathbf{k} space of the valence band maximum depends on the number of p orbitals per unit cell that contribute to the carbon π system. In P3HT there are eight such carbon p orbitals, meaning that there are eight electrons that fill four π bands. In PBTTT, with its fused thiophene rings, there are 14 C p orbitals per cell in the carbon π system. Thus there are 14 electrons that fill seven π bands. Because of band folding, when the number of filled π bands is even, the maximum energy occurs at the Γ point, and when the number of filled π bands is odd, the maximum will occur at the zone edge.

The band structure for PBTTT-C6 is shown in Fig. 5(a). Two hole bands, $H1$ and $H2$, and two electron bands, $E1$ and $E2$, are shown. In a field-effect transistor holes will populate the $H1$ band. As found also for other for polymers,^{9,14,24-27} the dispersion of the hole and electron states is larger along the polymer axis than in the transverse direction. Note that the valence band maximum is located at the zone edge (J) rather than at the zone center (Γ) for the reasons discussed above. The calculations show that there is a dispersion of the $H1$ band by 0.67 eV in the π -stacking direction, from $J = (\pi/c, 0)$ to $K = (\pi/c, \pi/b)$. From the band structure we determine the effective mass of the holes for transport in the direction of the π stacking to be $m_{\pi\pi}^*/m = 1.61$. The hole effective mass for transport along the polymer axis is $m_c^*/m = 0.10$. In models where the mobility is proportional to $(1/m^*)^{5/2}$, the mobility will be three orders of magnitude larger along the chain axis than in the π -stacking direction. In reality the mobility along the chain will be limited by the finite length of the polymers.

The electronic structure for P3HT is shown in Fig. 5(b). In contrast to PBTTT, the valence band maximum in P3HT is located at the Γ point. We find a downward dispersion of the $H1$ band by 0.62 eV in the π -stacking direction, from Γ to J' . Along the polymer chain axis, from Γ to J , the dispersion of the $H1$ band is 1.9 eV. This dispersion is similar to the energy dispersion of the corresponding band calculated for a herringbone-stacked bulk crystal of unsubstituted polythiophene.²⁵ The effective hole masses for transport in the π -stacking direction and along the chains are $m_{\pi\pi}^*/m = 1.74$ and $m_c^*/m = 0.14$. These masses are similar to the corresponding ones obtained for PBTTT.

The tilt of the conjugated chains has a large effect on the electronic structure. For perfectly cofacial P3HT ($\theta=0$) the width of the $H1$ band in the π -stacking direction is found to be 0.82 eV. Thus the rotation of the backbone reduces the

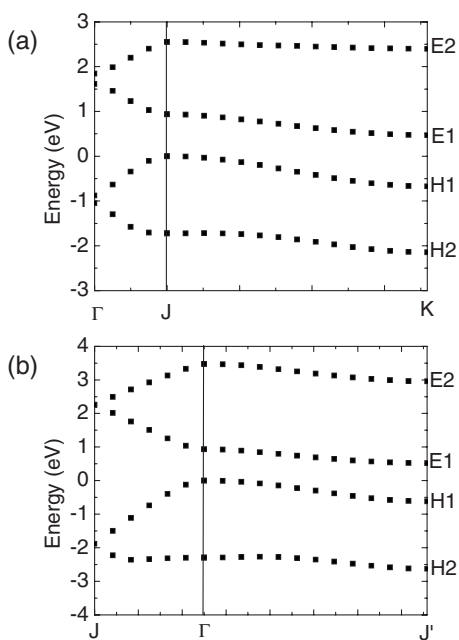


FIG. 5. (a) Band structure of PBTTC6. The valence band maximum occurs at J. (b) Band structure of P3HT. The valence band maximum occurs at Γ . The bands $H1$ and $H2$ are the topmost valence bands. The bands $E1$ and $E2$ are the lowest energy conduction bands. The points in the two-dimensional Brillouin zone are labeled as follows: $\Gamma=(0,0)$, $J=(\pi/c,0)$, $J'=(0,\pi/b)$, and $K=(\pi/c,\pi/b)$. The Γ - J direction is along the polymer axis. The Γ - J' and J - K directions correspond to dispersion in the π -stacking direction. In the calculations for P3HT, $b=7.1$ bohr and $c=14.4$ bohr. In the calculations for PBTTC6, $b=7.1$ bohr and $c=25.5$ bohr. The energy gap between occupied and empty states in these density functional calculations is expected to be substantially less than the experimental value.

bandwidth in the π -stacking direction by 25%. The dispersion along the chains is not affected significantly by the tilt; it is reduced by 3%. Within the local density approximation that is employed here, the energy band gap is increased from ~ 0.1 eV to ~ 0.5 eV by the rotation of the backbone. Thus, inclusion of the rotation is important for an accurate calculation of the optical properties.

C. Mobility estimate

One may gain some insight into the factors which govern the intrinsic mobility, and estimate an upper bound on the mobility of single crystals, by employing the acoustic deformation potential scattering model discussed by Karl.²⁸ In this picture the temperature-dependent mobility resulting from scattering by acoustic phonons is given by

$$\mu = \frac{2.45\pi\hbar^4 B e}{\epsilon_{ac}^2 (3kT)^{3/2} (m^*)^{5/2}}. \quad (1)$$

To calculate the mobility within this model we require the effective mass for the holes (m^*/m), the deformation potential (ϵ_{ac}), and an elastic constant (B). These are obtained from calculations of the band structure and total energy as a function of b , the interchain spacing.⁹ The deformation po-

tential $\epsilon_{ac}=b(dE_{vbm}/db)$, is obtained by calculating the energy of the valence band maximum, relative to the potential in the vacuum region, as a function of b . In the calculations of the deformation potential the d spacing, the distance between the sheets, is taken to be 44 bohr so that there is a clearly defined vacuum region. This model assumes that scattering results from long wavelength fluctuations in the π - π stacking distance. For PBTTC6 we obtain $(m^*/m)=1.61$, $\epsilon_{ac}=2.94$ eV, and $B=5.0\times 10^{-2}$ eV/ \AA^3 . For P3HT we have $(m^*/m)=1.74$, $\epsilon_{ac}=2.28$ eV, and $B=7.6\times 10^{-2}$ eV/ \AA^3 .

Inserting these parameters into Eq. (1) leads to a room temperature mobility for transport in the π -stacking direction of 15 cm^2/Vs for PBTTC6 and 31 cm^2/Vs for P3HT.²⁹ According to this model, the mobility within a *crystalline* region of P3HT would be larger than that in PBTTC6. This is opposite to what is measured in the *polycrystalline* material in thin-film transistors, where the effective mobility in PBTTC6 is ~ 0.6 cm^2/Vs and that of P3HT is ~ 0.1 cm^2/Vs . This indicates that the superior effective mobility in PBTTC6 transistors does not arise from higher intrinsic mobility within the crystalline regions, but from another factor, such as the increased mesoscopic ordering observed in PBTTC6.⁵

It is interesting to note that the estimated mobility in the π -stacking direction for crystalline PBTTC6 and P3HT is of magnitude similar to that measured within *single crystals* of small molecule organic semiconductors such as rubrene, where a room temperature mobility around 15–20 cm^2/Vs has been reported.³⁰ However, in the polycrystalline material employed in polymer thin-film-transistor devices, the mobility is limited by the size of the crystalline regions, and the requirement of transport through disordered regions at the edges of the grains.⁹ It is therefore not surprising that the mobility calculated by assuming a perfect crystal is not achieved in thin-film transistors. It seems likely that transport from one grain to another is dominated by a limited number of sites at which the coupling is large. For intergrain transport to occur it will be beneficial if the carrier can travel both along the chains and transverse to the chain in order to find these optimal coupling sites. For this reason hole delocalization is important.

D. Interdigitation and crystal stability

DeLongchamp *et al.* have found experimental evidence that the alkyl side chains in PBTTC6 exhibit interdigitation.⁷ To quantify the extent to which interdigitation impacts the stability, we performed calculations for PBTTC6 with a large spacing between neighboring sheets and with interdigitated chains. A monoclinic cell is employed: The unit cell vectors are $\mathbf{a}=(d,0,c/4)$, $\mathbf{b}=(0,b,0)$, and $\mathbf{c}=(0,0,c)$. Structures with $d=24$ bohr (fully interdigitated) and $d=34$ bohr (minimal interdigitation) are shown in Fig. 2. The total energy was calculated for various values of d , and the results are plotted in Fig. 6(a). One sees that there is a substantial energy reduction resulting from interdigitation, and that it is essentially complete. However, if the hydrogen atoms on the end of the alkyl chain get too close to the backbone of a neighboring polymer, then the energy in-

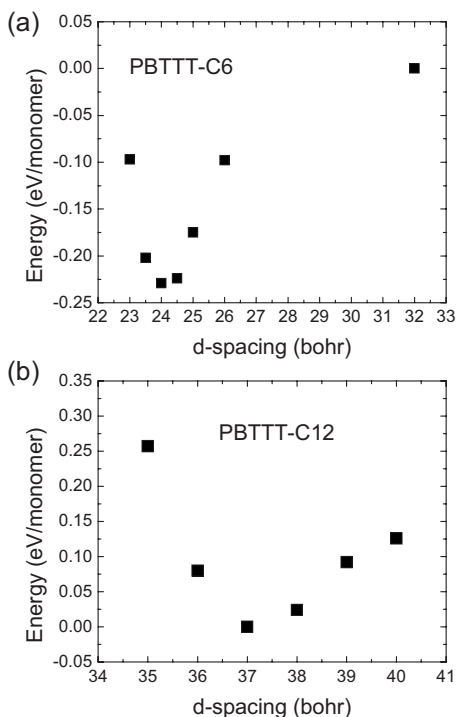


FIG. 6. (a) The energy vs d spacing for PBTTT-C6 is shown. Interdigitation of the alkyl chains is seen to be energetically favorable. Interdigitated structures corresponding to $d=24$ and $d=34$ bohr are shown in Fig. 2. (b) The energy vs d spacing for PBTTT-C12.

creases, as seen in the energy values for d less than 24 bohr. The optimum distance between the two-dimensional sheets in these calculations for PBTTT-C6 is approximately 24 bohr.

One can employ this result to predict the spacing for other alkyl chain lengths. The spacing for PBTTT-C n having *all-trans* side chains with n carbon atoms should be given roughly by $d(n)=d(6)+(n-6)\Delta d$, where $d(6)$ is the equilibrium d spacing for PBTTT-C6 and Δd is the computed average distance between alkyl-chain C atoms in the direction normal to the sheets. The d spacing increases because additional CH₂ units are inserted into the side chains. The value of Δd corresponds to a second-nearest-neighbor distance $\lambda=4.77$ bohr and an alkyl-chain orientation angle with respect to the normal of $\alpha=23^\circ$; $\Delta d=\frac{1}{2}\lambda\cos(\alpha)=2.20$ bohr. This model for predicting the lamellar spacing makes the assumption that the orientation angle of the alkyl chains is independent of n , and that the separation between the end of the alkyl chain and the backbone is the same as for the PBTTT-C6 structure. For PBTTT-C n , with n

$=(8, 10, 12, 14, 16)$ the model predicts $d=(28.4, 32.8, 37.2, 41.6, 46.0)$ bohr. Differences between the model and experiment are most likely to be a consequence of variations in α rather than λ . Detailed studies of d spacing as a function of n would be interesting, as deviations from this type of linear model could yield further insight into the structure of these materials.

To test the model, calculations were performed for PBTTT-C12. The energy was calculated for values of d between 35 and 40 bohr. The minimum in energy occurs for d equal to 37 ± 1 bohr (19.6 ± 0.5 Å), as seen in Fig. 6(b). This is in agreement with the model, which gives $d(12)=37.2$ bohr. The result is in agreement with the experimentally determined values of 37.0 bohr (19.6 Å) and 36.3 bohr (19.2 Å).^{5,10} The difference between the calculated d spacing and the experimental d spacing is less than 0.5 Å. Nevertheless, some caution is in order. First, a complete exploration of the landscape of possible alkyl side chains orientations has not been attempted. In addition, the DFT calculations do not treat the van der Waals interactions in a formally correct way,³¹ and these may play an important role in determining the weak nonbonding interactions between the alkyl side chains. Nevertheless, it is clear from experiment that interdigitation does occur in PBTTT,⁷ and these calculations indicate that it contributes to the stability.

IV. SUMMARY

In summary these calculations indicate that the planes containing the conjugated rings in P3HT, PQT-C6, and PBTTT-C6 are tilted by $\sim 23^\circ$. This rotation contributes substantially to the stability, and has important consequences for the electronic structure: It reduces the electron and hole bandwidths, and opens up the energy gap between occupied and empty states. Estimates of the mobility expected in crystalline PBTTT and P3HT suggest that the comparatively higher mobility measured in polycrystalline PBTTT could be a result of improved mesoscopic ordering and not necessarily a result of the differences in the local atomic structures. The calculations indicate that interdigitation of the alkyl chains in PBTTT is energetically favorable. Therefore, polymers that are able to interdigitate maximally may be expected to exhibit a greater structural stability.

ACKNOWLEDGMENTS

The author is grateful to A. Salleo, R. A. Street, M. L. Chabinye, and D. M. DeLongchamp for helpful discussions. This work was supported by the AFOSR under Grant No. FA9550-06-1-0302.

¹R. D. McCullough, Adv. Mater. (Weinheim, Ger.) **10**, 93 (1998).

²Z. Bao, A. Dodabalapor, and A. J. Lovinger, Appl. Phys. Lett. **69**, 4108 (1996).

³H. Sirringhaus *et al.*, Nature (London), **401**, 685 (1999).

⁴B. S. Ong, Y. Wu, P. Liu, and S. Gardner, J. Am. Chem. Soc. **126**, 3378 (2004).

⁵I. McCulloch *et al.*, Nat. Mater., **5**, 328 (2006).

⁶M. Heeney, C. Bailey, K. Genevicius, M. Shkunov, D. Sparrowe,

- S. Tierney, and I. McCulloch, *J. Am. Chem. Soc.* **127**, 1078 (2005).
- ⁷D. M. DeLongchamp, R. J. Kline, E. K. Lin, D. A. Fischer, L. J. Richter, L. A. Lucas, M. Heeney, I. McCulloch, and J. E. Northrup, *Adv. Mater. (Weinheim, Ger.)* **19**, 833 (2007).
- ⁸A. Salleo, T. W. Chen, A. R. Volkel, Y. Wu, P. Liu, B. S. Ong, and R. A. Street, *Phys. Rev. B* **70**, 115311 (2004).
- ⁹R. A. Street, J. E. Northrup, and A. Salleo, *Phys. Rev. B* **71**, 165202 (2005).
- ¹⁰M. L. Chabinyc, M. F. Toney, R. J. Kline, I. McCulloch, and M. Heeney, *J. Am. Chem. Soc.* **129**, 3226 (2007).
- ¹¹J.-F. Chang, J. Clark, N. Zhao, H. Sirringhaus, D. W. Breiby, J. W. Andreasen, M. M. Nielsen, M. Giles, M. Heeney, and I. McCulloch, *Phys. Rev. B*, **74**, 115318 (2006).
- ¹²R. J. Kline, M. D. McGehee, E. N. Kadnikova, J. Liu, and J. M. J. Frechet, *Adv. Mater. (Weinheim, Ger.)* **15**, 1519 (2003).
- ¹³R. Osterbacka, C. P. An, X. M. Jiang, and Z. V. Vardeny, *Science* **287**, 839 (2000).
- ¹⁴D. Beljonne, J. Cornil, H. Sirringhaus, P. J. Brown, M. Shkunov, R. H. Friend, and J.-L. Bredas, *Adv. Funct. Mater.* **11**, 29 (2001).
- ¹⁵M. Bockstedte, A. Kley, J. Neugebauer, and M. Scheffler, *Comput. Phys. Commun.* **107**, 187 (1997).
- ¹⁶W. Kohn and L. J. Sham, *Phys. Rev.* **140**, 1133 (1965).
- ¹⁷N. Troullier and J. L. Martins, *Phys. Rev. B* **43**, 1993 (1991).
- ¹⁸D. M. Ceperley and B. J. Alder, *Phys. Rev. Lett.* **45**, 566 (1980).
- ¹⁹J. E. Northrup, M. L. Tiago, and S. G. Louie, *Phys. Rev. B* **66**, 121404(R) (2002).
- ²⁰J. E. Northrup and M. L. Chabinyc, *Phys. Rev. B* **68**, 041202(R) (2003).
- ²¹J. T. Sadowski, G. Sazaki, S. Nishikata, A. Al-Mahboob, Y. Fujikawa, K. Nakajima, R. M. Tromp, and T. Sakurai, *Phys. Rev. Lett.* **98**, 046104 (2007).
- ²²M. O. Sinnokrot, E. F. Valeev, and C. D. Sherrill, *J. Am. Chem. Soc.* **124**, 10887 (2002).
- ²³K. Hummer, P. Puschnig, and C. Ambrosch-Draxl, *Phys. Rev. B* **67**, 184105 (2003).
- ²⁴J.-W. van der Horst, P. A. Bobbert, and M. A. J. Michels, *Phys. Rev. B* **66**, 035206 (2002).
- ²⁵A. Ferretti, A. Ruini, G. Bussi, E. Molinari, and M. J. Caldas, *Phys. Rev. B* **69**, 205205 (2004).
- ²⁶M. Rohlfing and S. G. Louie, *Phys. Rev. Lett.* **82**, 1959 (1999).
- ²⁷J.-W. van der Horst, P. A. Bobbert, M. A. J. Michels, G. Brocks, and P. J. Kelly, *Phys. Rev. Lett.* **83**, 4413 (1999).
- ²⁸N. Karl, in *Organic Electronic Materials*, edited by R. Farchioni and G. Grosso (Springer, Berlin, 2001).
- ²⁹The corresponding mean free paths are 14 and 30 Å.
- ³⁰V. Podzorov, E. Menard, A. Borissov, V. Kiryukhin, J. A. Rogers, and M. E. Gershenson, *Phys. Rev. Lett.* **93**, 086602 (2004).
- ³¹W. Kohn, Y. Meir, and D. E. Makarov, *Phys. Rev. Lett.* **80**, 4153 (1998).